Powder Technology 267 (2014) 111–118

Contents lists available at ScienceDirect

Powder Technology

journal homepage: www.elsevier.com/locate/powtec

Synthesis of cordierite by dolomite and kaolinitic clay chlorination. Study of the phase transformations and reaction mechanism

P. Orosco [a,b,*], M. del C. Ruiz [a], J. González [a,c]

[a] Instituto de Investigaciones en Tecnología Química (INTEQUI–CONICET), Chacabuco y Pedernera, 5700, San Luis, Argentina
[b] Facultad de Química, Bioquímica y Farmacia, Universidad Nacional de San Luis, Chacabuco y Pedernera, 5700 San Luis, Argentina
[c] Instituto de Ciencias Básicas, Universidad Nacional de Cuyo, Parque General San Martín, 5500 Mendoza, Argentina

ARTICLE INFO

Article history:
Received 13 December 2013
Received in revised form 20 June 2014
Accepted 6 July 2014
Available online 12 July 2014

Keywords:
Cordierite
Chlorination
Chemical synthesis
Thermogravimetric analysis

ABSTRACT

The focus of analysis in this work has been the study of the synthesis of cordierite using a pyrometallurgical route which involved thermal treatment in a chlorine atmosphere of a kaolinitic clay and dolomite mixture as raw material. The reaction mechanism was also investigated. Isothermal and non-isothermal chlorination assays were conducted in experimental equipment adapted for working in corrosive atmospheres. The temperature effect on the reactions yielding cordierite were studied. Both reagents and products were analyzed by X-ray diffraction (XRD), X-ray fluorescence (XRF), scanning electron microscopy (SEM), and electron probe microanalysis (EPMA). The experimental results have shown that cordierite starts to be produced at 700 °C, and that the elimination of iron, which is present as an impurity, begins at about 700 °C. The most favorable chlorination temperature was 900 °C, since at this temperature a selective production of cordierite and an efficient elimination of iron were achieved.

1. Introduction

Cordierite is a magnesium aluminosilicate composed of a ternary system of oxides ($MgO:Al_2O_3:SiO_2$) in a 2:2:5 ratio. In nature, it generates as a product of the thermal metamorphosis of clay rocks; crystallizes in an orthorhombic system, and it has a pseudo-hexagonal habit; its density is 2.53 g/cm^3, and its fusion point is 1470 °C [1–3].

This ceramic material has been the focus of attention over the last years due to its properties, such as low thermal expansion coefficient, low dielectric constant, low dielectric loss, high specific resistivity, high thermal shock resistance, and high temperature stability. These properties make cordierite an ideal material for use in the electronic industry [4,5]. One of the most significant applications of cordierite is as catalysts support in diverse processes, some of which can be found in the petrochemical industry, the selective reduction of alcohol, the control of automobile emissions, and the control of volatile organic compounds.

Cordierite is a mineral which is not abundant, or pure enough in nature; for this reason, it is necessary to synthesize it. The typical processes for cordierite synthesis are: sol–gel technique, glass crystallization technique, and reactions in solid state. The latter two techniques use natural mineral resources as raw material [5,6]. In industry, the production of cordierite is carried out by the process of reactions in solid state.

Several investigations [7–11] have been conducted in the last two decades with the aim of reducing the formation temperature of cordierite. These studies were carried out with the purpose of reducing the cost of processing, and improving the properties of cordierite. To this end, auxiliary minerals such as bismuth oxide and phosphorus pentoxide were used in the process of reactions in solid state [7,8]. The sol–gel method using aluminum acetate gel, tetraethyl orthosilicate, magnesium acetate solution, ethanol and phenol–formaldehyde resin [9] and non-hydrolytic sol–gel route [10] were investigated. Also the mechanical activation method to reduce the formation temperature of cordierite has been reported [11]. However, cordierite has not been possible to synthesize below 1000 °C by using the above mentioned methods so far.

A few researchers have been able to produce the pure cordierite phase, but only by using high synthesis temperatures which range from 1300 °C to 1400 °C [3,4]. Different studies [5,12–14] have shown that cordierite can be crystallized at about 950 °C by using the glass crystallization technique. However, this technique requires an additional energetic cost for the previous treatment applied to the raw materials with the aim of melting the precursors.

The presence of some impurities increases the thermal expansion coefficient and confers the color to the cordierite. Iron which is generally present in cordierite is one of the main elements increasing the thermal expansion coefficient, and it is also responsible for giving the material an undesirable reddish color, as well as for reducing its refractory properties [15,16]. Vitreous silica formed during the processing of phyllosilicates (talc, kaolin, kaolinitic clay, etc.), which are generally used for obtaining cordierite, also produces a considerable increase in

* Corresponding author at: Instituto de Investigaciones en Tecnología Química (INTEQUI-CONICET), Chacabuco y Pedernera -5700- San Luis, Argentina. Tel: +542664426711; fax: +542664426711.
E-mail address: porosco@unsl.edu.ar (P. Orosco).

http://dx.doi.org/10.1016/j.powtec.2014.07.009
0032-5910/

the thermal expansion coefficient [6,17]. Therefore it is necessary to remove or to avoid the presence of iron and vitreous silica.

The pyrometallurgic process of chlorination can be used to reduce the temperature of cordierite synthesis and eliminate the impurities which affect the thermal expansion coefficient, color and refractory properties. This method has been effectively used in the extraction of various metals from oxides and minerals in the last decades. This is due to the high reactivity of the chlorinating agent, the selectivity of the reaction, the simple treatment of effluents, and the low cost of the processes. Further, various studies have reported the effect of thermal treatment in chlorine atmosphere on the phase transformations of some materials, such as oxides and minerals, as well as the fact that the formation of intermediate chlorinated compounds favors the generation of products whose obtention by other means requires a more energetic treatment [18–20]. Although this information, there are no bibliographic data about the cordierite synthesis by mixture of minerals chlorination.

The previous studies referred to phase transformations during the thermal treatments of the chlorination of refractory clays and talc provided important information to investigate the synthesis of cordierite from the mixture of kaolinitic clay and dolomite [21,22].

This study has been devoted to studying the mechanism of chlorination of a mixture of kaolinitic clay and dolomite with chlorine gas in order to synthesize cordierite. The phase transformations occurring during the chlorination were also investigated. The knowledge of the process that occurs when the mixture is calcined in Cl_2 is crucial to optimize the synthesis of cordierite and improve the properties of this ceramic material. This study was done in order to reduce the working temperature of cordierite synthesis, exploit Argentinian natural resources, and eliminate the impurities that affect the thermal expansion coefficient, color, and refractory properties.

2. Materials and methods

2.1. Materials

The solid reagent used in the synthesis of cordierite by chlorination was a mixture of dolomite and kaolinitic clay, both of Argentine origin. The mixture of these minerals, denominated M, was prepared in a ratio of the 70% w/w of kaolinitic clay and 30% w/w of dolomite. This ratio was selected taking into account the stoichiometric composition of the cordierite and the impurities contained in the starting minerals. The preparation of the mixture was made in a disk mill, and the mixing time was 4 min.

Table 1
Chemical composition (w/w%) of the starting minerals and the M sample.

	Mineral		Sample
	Kaolinitic clay	Dolomite	M
Al_2O_3	28	–	20
SiO_2	53	–	36
Fe_2O_3	3.5	–	2.5
CaO	1.3	33.2	8.6
MgO	1.2	19.5	7.2
TiO_2	0.7	-	0.5
LOI	11.85	48.23	14.2

The primary minerals which are present in the mixture under study were identified by X-ray diffraction (XRD). The diffractogram of the mixture of dolomite and kaolinitic clay (Fig. 1) shows the presence of kaolinite (JCPDS 89–6538), dolomite (JCPDS 89–5862), calcite (JCPDS 86–2340) and quartz (JCPDS 89–8939).

The chemical composition of the minerals and the M sample were determined by X-ray fluorescence (XRF). The results obtained are presented in Table 1. The table shows that the mixture contains iron, which comes from the impurities of the clay. Iron can be found as either a phase separate from kaolinite or adsorbed on its surface as colloidal iron in the form of hematite (Fe_2O_3), limonite (FeOOH), or ferric hydroxide ($Fe(OH)_3$) [19,21].

In order to determine some of the mineral phases of iron present in the mixture, an analysis was performed by scanning electron microscopy (SEM) and electron probe microanalysis (EPMA).

SEM image obtained with back-scattered electrons is shown in Fig. 2. The brilliant particle indicated with an arrow was analyzed by EPMA (Table 2). The composition of hematite has also been reported in the table with comparative purpose. The composition of this particle suggests that it is probably a hematite particle.

The gasses used in the different assays were chlorine 99.5% v/v as reactive gas, provided by Cofil, and nitrogen 99.99% v/v as diluent and purge gas, provided by Air Liquid.

2.2. Equipment

The experimental chlorination assays were performed in a thermogravimetric system designed in our laboratory [23]. The dispositive is provided of a reactor of quartz placed inside an electric furnace equipped with a temperature controller. The sample was contained in a quartz

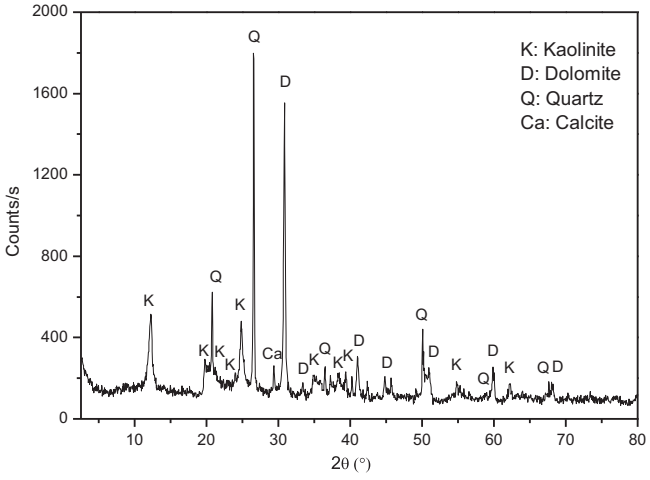

Fig. 1. Diffractogram of the M sample.

Fig. 2. SEM micrograph corresponding to particles of the M sample.

Table 2
EPMA analysis, in atomic %, corresponding to the particle marked in Fig. 2.

Particle	Mg		Al		Si		Fe		Ca		O	
	T	E	T	E	T	E	T	E	T	E	T	E
⇨	–	–	–	–	–	–	59.33	69.94	–	–	40.64	30.06

T: Theoretical composition corresponding to hematite formula.
E: Experimental data.

crucible which was introduced inside the reactor. The temperature was measured with a chromel–alumel thermocouple to within ±5 K. The measurement system of mass is an analytical balance (Mettler Toledo AB204-S/FACT, maximum sensitivity of 0.0001 g) connected to an automatic data logger.

Chlorine was introduced to the inlet of the reactor of quartz through teflon tubing. Mass flow meters and metering valves were used to control the flow rate.

The X-ray diffraction (XRD) analysis of reactants and reaction products was performed on Rigaku D-Max-IIC equipment with Cu Kα, operated at 35 kV and 30 mA. Scanning electron microscopy (SEM) and electron probe microanalysis (EPMA) characterizations were carried out using a LEO 1450VP microscope equipped with an energy dispersive X-ray (EDS) spectrometer (EDAX Genesis 2000). The composition of the kaolinitic clay and dolomite mixture and the chlorination residues was determined by X-ray fluorescence (XRF) with Philips PW 1400 equipment.

2.3. Procedure

Isothermal and non-isothermal chlorination assays were carried out using masses of approximately 1 g of powder sample. For the different thermal treatments, flows of 50 ml/min of N_2 and 100 ml/min of Cl_2/N_2 (50% v/v) were used.

2.4. Procedure for non-isothermal chlorination

1. The quartz crucible was filled with starting mixture and carefully placed into the center of the reactor.
2. A linear heating program was set from at a heating rate of 5 °C/min from 20 °C to 1000 °C, the dispositive switched on, and the gaseous mixture Cl_2/N_2 fed into the reactor.
3 Upon attainment of the final temperature, chlorine supply was cut off.
4 The sample was taken out from the reactor and cooled down.

2.5. Procedure for isothermal chlorination

1. The reaction temperature was set, the furnace switched on, and N_2 fed into the reactor. The heating rate was 5 °C/min.
2. The quartz crucible was filled with starting mixture.
3. Upon attainment of the working temperature, the quartz crucible was carefully placed into the center of the reactor.
4. Cl_2 was fed into the reactor, generating the mixture of Cl_2/N_2 (50% v/v).
5. The sample was kept at this temperature for 5 min.
6. Upon attainment of the reaction time, Cl_2 supply was cut off.
7. The sample was taken out from the reactor and cooled down.

The reaction period was chosen to account the time required to observe changes of mass registered in non-isothermal chlorination assay.

2.6. Washing and filtration of the chlorination residues

All the residues of these chlorination assays were subjected to processes of washing and filtration with hot water in order to remove calcium and magnesium chloride present in the chlorinated sample. Then, the residues obtained were dried in an oven at 100 °C. In some cases, the filtering liquid was evaporated in the oven at 100 °C.

The washed and dried residues of filtration and solids from the evaporation of filtering liquid were analyzed by X-ray diffraction.

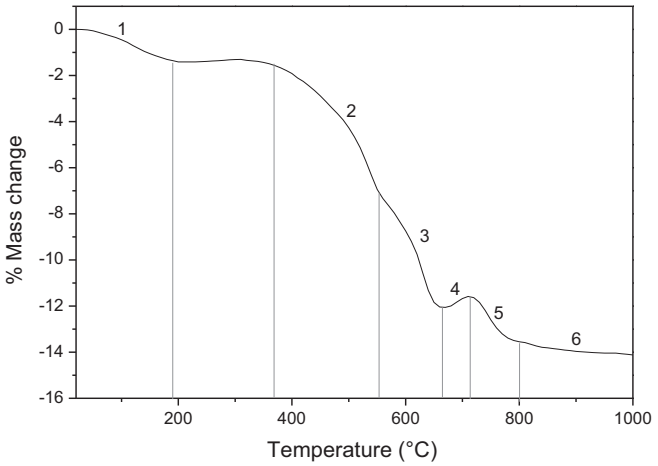

Fig. 3. Thermogram corresponding to the M sample calcined in Cl_2/N_2.

2.7. Additional trials

Isothermal chlorination assays were carried out between 700 and 1000 °C in Cl_2/N_2 (50% v/v) atmosphere during 120 min to determine the temperature range for which the selective formation of cordierite is accomplished.

3. Results and discussion

The results of the non-isothermal treatment of the M sample in Cl_2/N_2 current are presented in Fig. 3. The thermogravimetric curve of the sample presents six zones of mass change. The first three zones, together with the fifth and sixth, correspond to the phenomena which produce mass losses, whereas a mass gain occurs in the fourth zone. The first zone of mass change (Fig. 3) occurs in the range between 50 and 190 °C. The second zone can be seen between 370 and 550 °C. The third region can be observed in the interval between 550 and 660 °C. At temperatures ranging between 660 and 710 °C, a region of mass increase is observed. The mass changes observed in the fifth and sixth zone between 710 and 800 °C, and between 800 and 1000 °C, respectively, correspond to a balance between mass gain and loss occurring in the sample as a consequence of the phenomena which take place in each temperature interval.

Isothermal assays were conducted in the temperature range between 500 and 1000 °C, and then the residues were analyzed by XRD with the purpose of determining the phenomena which take place during the thermal treatments in Cl_2, to which the sample under study was subjected. Fig. 4 shows the diffractograms of the chlorination residues obtained at different temperatures for periods of 5 min.

3.1. First zone of mass change (50–190 °C)

The chlorination residue in this temperature interval was not analyzed by XRD, since the mass loss observed in the thermogram of

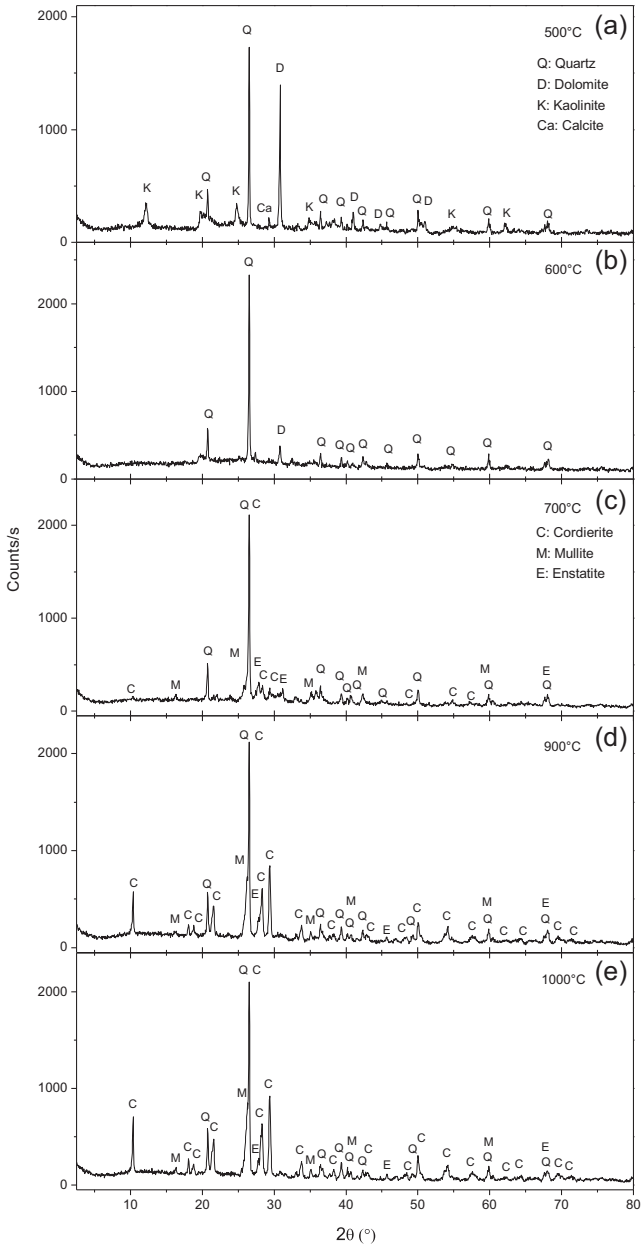

Fig. 4. Diffractograms of the chlorination residues of the M sample at different temperatures and periods of 5 min.

the sample corresponds to the elimination of the water physically adsorbed in the clay which is part of the mixture.

3.2. Second zone of mass change (370–550 °C)

This region corresponds to kaolinite dehydroxylation, according to reaction (1):

$$Al_2O_3.2SiO_2.2H_2O \rightarrow Al_2O_3.2SiO_2 + 2H_2O(g). \quad (1)$$

This phenomenon has been tested by the diffractogram of the residue corresponding to the calcined sample at 500 °C (Fig. 4a). The diffractogram shows a diminution in the intensity of characteristic diffraction peaks of kaolinite, which indicates partial dehydroxylation of this mineral.

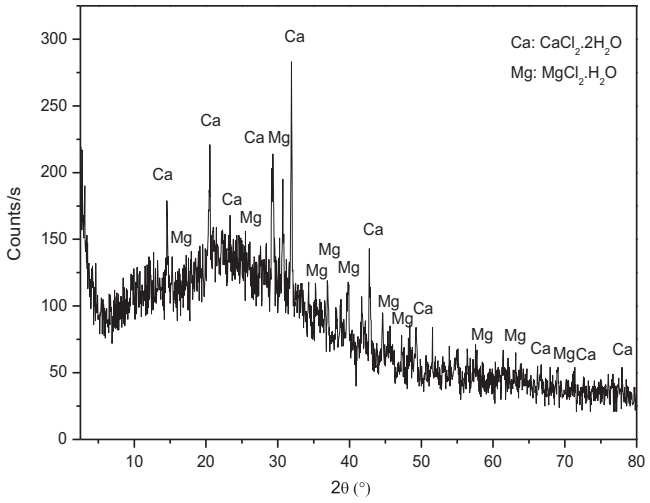

Fig. 5. Diffractogram of the solid from evaporation of filtering liquid obtained by washing of the chlorination residue of the M sample at 700 °C.

3.3. Third zone of mass change (550–660 °C)

The third region of mass loss observed in the thermogram of Fig. 3 corresponds to the thermal decomposition of dolomite:

$$CaMg(CO_3)_2 \rightarrow CaO + MgO + 2CO_2(g). \quad (2)$$

This can be deduced from the results shown in Fig. 4b, where a decrease in the intensity of typical peak of dolomite is observed as a result of dolomite partial decomposition. Lime and periclase phases, products of reaction (2), do not appear in the XRD pattern, probably because they are as amorphous phases. Decomposition of calcite, which accompanies dolomite as an impurity, is also produced in this stage.

3.4. Fourth zone of mass change (660–710 °C)

The phenomena that occur in this region are described below by using the diffractograms in Fig. 4c to e, and Fig. 5.

3.4.1. Stage 1: chemical interaction between lime and periclase, products of dolomite decomposition, and Cl_2 with formation of $CaCl_2$ and $MgCl_2$

The formation of $CaCl_2$ and $MgCl_2$ can be observed in Fig. 3 as a mass gain starting at 660 °C. The occurrence of this reaction was probed using the solid from evaporation of filtering liquid obtained by washing of the chlorination residue of the M sample at 700 °C. The XRD pattern of this solid (Fig. 5) shows the presence of calcium and magnesium chlorides (JCPDS 53–260 and 70–385), which are the products of the chlorination

Table 3
Contents of iron, expressed as Fe_2O_3, in the chlorination residues of the M sample at different temperatures and periods of 5 min.

Temperature (°C)	Fe_2O_3 (w/w%)	Extraction (%)
20	2.5	–
600	2.5	–
700	1.81	27.6
800	0.48	80.9
900	0.45	82.2
1000	0.38	84.6

of lime and periclase (reactions (3) and (4)):

$$CaO + Cl_2(g) \rightarrow CaCl_2 + 0.5O_2(g) \quad (3)$$

$$MgO + Cl_2(g) \rightarrow MgCl_2 + 0.5O_2(g). \quad (4)$$

The chlorides shown in Fig. 5 are hydrated because they suffer a hydration process after being extracted from the reactor.

The chlorination of lime and periclase then continues until 1000 °C, according to the data previously reported by Orosco et al. [22], who observed during the dolomite chlorination a mass increment between 800 and 1000 °C due to the production of $CaCl_2$ and $MgCl_2$.

3.4.2. Stage 2: synthesis of cordierite

Cordierite synthesis occurs through two steps. In the first, $MgCl_2$ and O_2, generated by chlorination of periclase and lime, react with metakolinite produced by kaolinite decomposition, forming mullite and enstatite:

$$3/4Al_2O_3.2SiO_2 + MgCl_2(l) + 1/2O_2(g) \rightarrow 1/4(3Al_2O_3.2SiO_2) + MgSiO_3 + Cl_2(g). \quad (5)$$

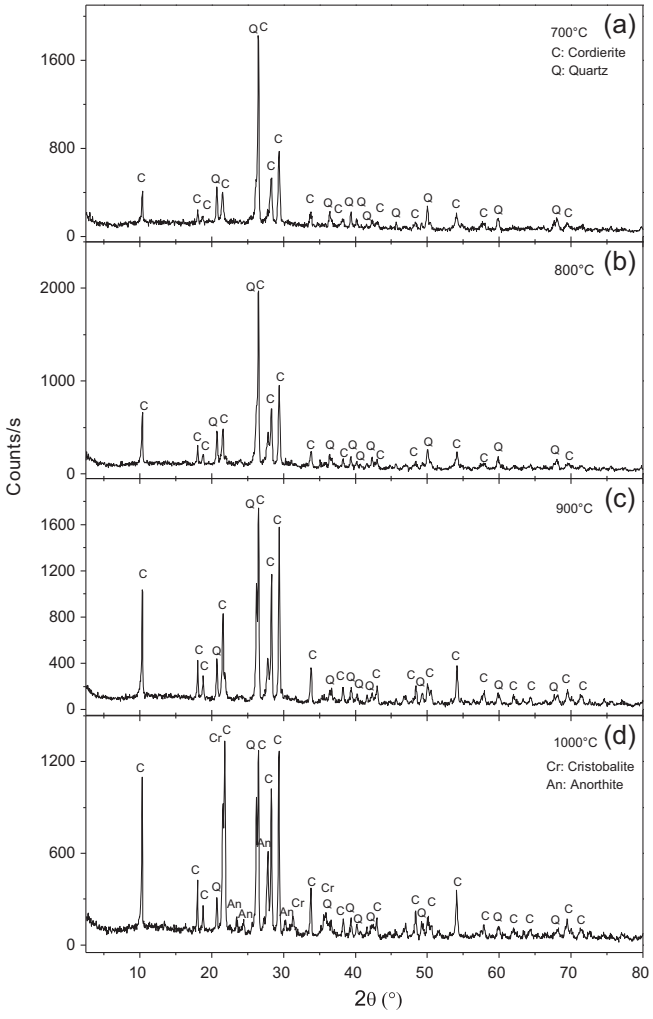

Fig. 6. Diffractograms of the chlorination residue of the M sample at different temperatures and periods of 120 min.

Table 4
Contents of iron, expressed as Fe_2O_3, in the chlorination residues of the M sample at different temperatures and periods of 120 min.

Temperature (°C)	Fe_2O_3 (w/w%)	Extraction (%)
20	2.5	–
600	2.46	1.6
700	0.58	76.8
800	0.37	85.2
900	0.29	88.4
1000	0.27	89.2

Subsequently, mullite and enstatite react with Cl_2 and produced cordierite, liquid $MgCl_2$ and O_2:

$$2/5(3Al_2O_3.2SiO_2) + 11/5MgSiO_3 + Cl_2(g) \rightarrow 3/5Mg_2Al_4Si_5O_{18} + MgCl_2(l) + 1/2O_2(g). \quad (6)$$

The occurrence of the reactions (5) and (6) has been verified by the diffractogram of the residue corresponding to the calcined sample at 700 °C (Fig. 4c). The figure shows the phases generated in the products. Mullite (JCPDS 89–2813), enstatite (JCPDS 76–2426) and cordierite (JCPDS 89–1487) phases can be observed in this figure, which confirms the proposed reaction mechanism for the synthesis of cordierite.

The synthesis of cordierite continues until the final investigated temperature. This can be inferred by comparing the diffractograms of the chlorination residues of the M sample, obtained between 700 and 1000 °C (Fig. 4c and e) since when the temperature increases the intensity of typical peaks of cordierite also increases.

At 700 °C the reactions (5) and (6) are possible due to the presence of $CaCl_2$, which changes the state of aggregation of $MgCl_2$. This assumption is based on the diagram of phases corresponding to Mg and Ca chlorides [24], which indicate that the Mg and Ca chlorides form an eutectic mixture with a point of fusion of 620 °C. Then, liquid $MgCl_2$ reacts with metakaolinite to yield mullite and enstatite (reaction (5)), which in turn react with chlorine to form cordierite (reaction (6)).

3.5. Fifth zone of mass change (710-800 °C)

The mass changes produced in this mass loss zone are due to two phenomena which are discussed below. The first one is the production of $MgCl_2$ and $CaCl_2$ as a consequence of chlorination of periclase and lime, respectively. The second one is produced by the volatilization of $FeCl_3$ formed during hematite chlorination:

$$1/3Fe_2O_3 + Cl_2(g) \rightarrow 2/3FeCl_3(g) + 1/2O_2(g). \quad (7)$$

Previous studies related to the reactivity of hematite with Cl_2 [19–21] have shown that the reaction starts at around 700 °C. The data from the iron analysis performed by XRF on the chlorination residues of the M sample at different temperatures and a reaction time of 5 min (Table 3), corroborate this phenomenon. According to the results obtained, it can be noted that a considerable extraction of Fe_2O_3 is produced between 700 and 800 °C. This is due to the fact that the hematite is being completely eliminated of the mixture in the form of $FeCl_3$ (g) [20,21].

The mass loss observed in the thermogram of this region proves that hematite chlorination (reaction (7)) rate is higher than that of periclase and lime (reactions (3) and (4)).

3.6. Sixth zone of mass change (800–1000 °C)

The sixth region of mass change, which can be seen in the chlorination thermogram of the sample, shows a slight mass loss. This is due to the fact that the chlorination reaction of the Fe (III) oxide adsorbed on the surface of kaolinite (reaction (7)), prevails over the production of $MgCl_2$ and $CaCl_2$ (reactions (3) and (4)). The reaction between this

iron oxide and Cl_2 has been previously observed during the deferrication of clays at temperatures between 800 and 1000 °C [20,21].

The content of iron in the residues of the M sample chlorinated at 800 and 1000 °C was measured by XRF (Table 3). The data obtained indicate that iron extraction in this temperature range is lower than the produced between 700 and 800 °C. These results can be explained taking account that the Fe (III) oxide is difficult to remove completely, since it is strongly adsorbed on the surface of minerals with laminar structure.

3.7. Conditions for selective formation of cordierite

The selective production of cordierite and the temperature range of synthesis have been experimentally deduced by chlorination assays of the M sample at different temperatures and a reaction time of 120 min, with a Cl_2/N_2 (50% v/v) flow, rate of 100 ml/min. The diffractograms of the chlorination residues are presented in Fig. 6.

Fig. 6a to c shows that in the temperature interval between 700 and 900 °C the phase generated is only cordierite, which confirms the selective formation of cordierite.

At 1000 °C $CaCl_2$ reacts with cordierite, thus producing anorthite, vitreous silica and $MgCl_2$, according to the following reaction:

$$CaCl_2(l) + 1/2Mg_2Al_4Si_5O_{18} \rightarrow CaAl_2Si_2O_8 + 1/2SiO_2 + MgCl_2(g). \quad (8)$$

The reaction (8) occurs as consequence of partial volatilization of the $MgCl_2$. This chloride can volatilize since it has a vapor pressure of 0.0097 atm at this temperature [23]. In the flow system used in this work, the volatile $MgCl_2$ leaves the reaction zone entrained by the chlorine stream, favoring the chlorination reaction of cordierite, and the formation of more volatile $MgCl_2$. Moreover, quartz coming from the initial sample, and vitreous silica which is a product of reaction (8), are transformed into cristobalite. These phenomena are corroborated by the diffractogram of Fig. 6d, where anorthite (JCPDS 76–948) and cristobalite (JCPDS 77–1317) phases appear.

The data of extraction of iron corresponding to the chlorination assays performed in the conditions mentioned below are showed in Table 4.

According to these results, the optimum temperature of chlorination aimed to synthesize cordierite from dolomite and kaolinitic clay is 900 °C; this is because at this temperature, an efficient remotion of iron is achieved, and the chlorination of cordierite does not occur.

Purity of cordierite was determined applying the RIR (relative intensity ratio) method by using the diffraction data of the solid obtained after washing and filtering the sample chlorinated at 900 °C for 120 min.

The results indicate that the purity of cordierite is 65%; this due to the fact that quartz originally contained in M remains in the chlorinated residue.

The yield of the reaction, with respect to solid reactants, was estimated through Eq. (9):

$$Y(\%) = \left[\frac{M_F P_C}{M(W_K + W_D)}\right] \times 100 \quad (9)$$

Where Y is the yield of reaction (%); M_F is the mass of the washed and filtered residue (g); P_C is the purity of cordierite; M is the mass of M (g); W_K is the content of kaolinitic clay in M (mass fraction) and W_D is the content of dolomite in M (mass fraction).

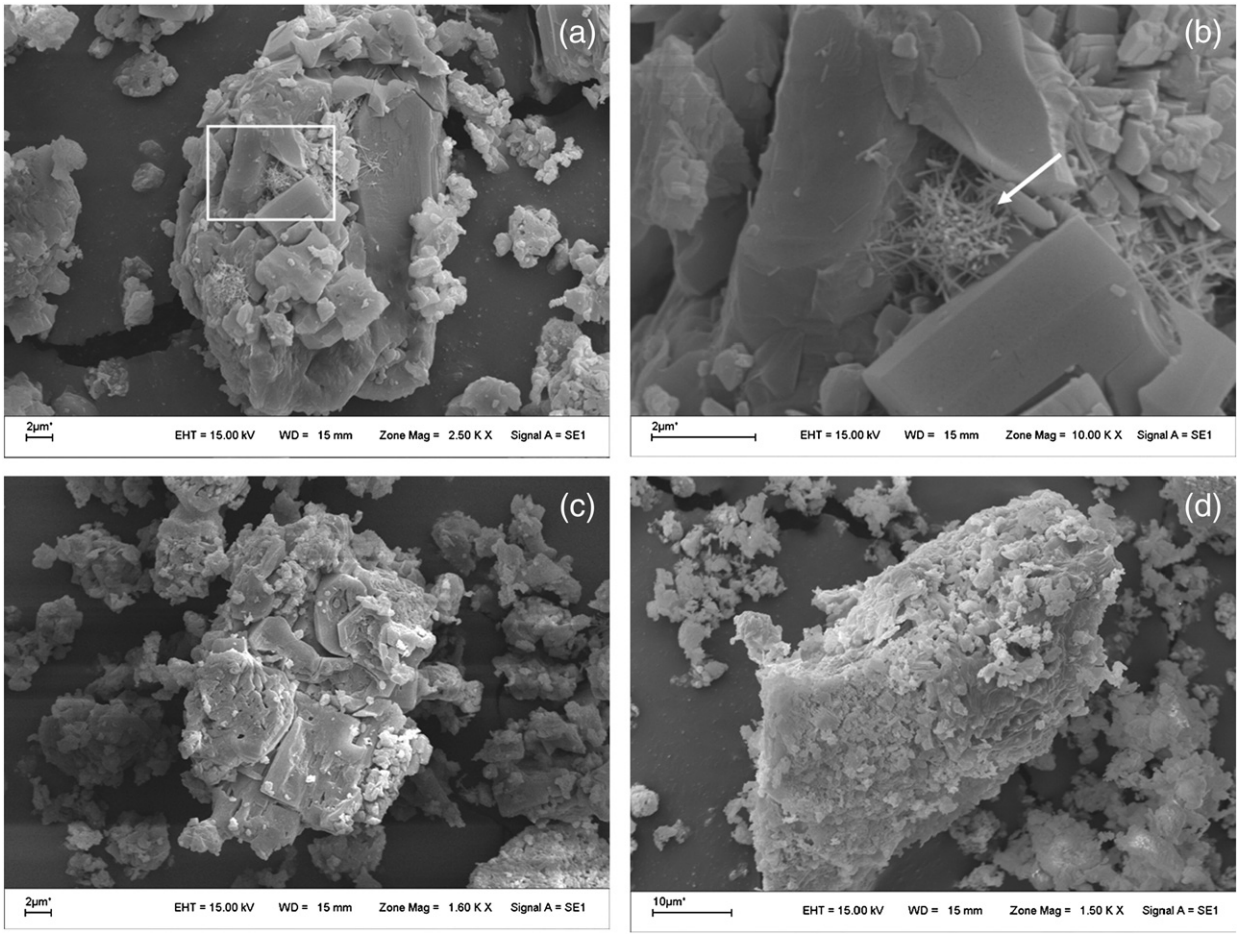

Fig. 7. SEM micrograph corresponding to particles of the M sample calcined in Cl_2/N_2: (a) calcination at 700 °C for 5 min, (b) amplified image of the particle marked in Fig. 1a, (c) calcination at 700 °C for 120 min, and (d) calcination at 900 °C for 120 min.

Table 5
EPMA analysis, in atomic %, corresponding to particles present in Fig. 7.

Temperature (°C)	Time (min)	Mg		Al		Si		O	
		T	E	T	E	T	E	T	E
700	15	–	–	38	34.74	13.18	15.32	48.82	48.51
	120	8.31	8.60	18.45	24.19	24.01	27.49	49.23	39.72
900	120	8.31	9.64	18.45	18.12	24.01	28.78	49.23	43.47

T: Theoretical composition corresponding to mullite (Fig. 7b) and cordierite (Fig. 7c and d) formulas.
E: Experimental data.

The values of W_K and W_M were calculated using data from Tables 1 and 2.

The yield estimated by Eq. (7) is 45%, which means that 45 g of cordierite is obtained from each 100 g of sample. The other products formed are $MgCl_2$(l), $CaCl_2$(l), CO_2(g), O_2(g) and H_2O(g).

Comparing the results of the different synthesis methods, it can be infer that the chlorination process proposed in this work is as selective as the processes of reactions in solid state [6–8] and glass crystallization [5,12–14] and it is more selective than sol–gel [9], non-hydrolytic sol–gel [4,10], and mechanical activation methods [11]. With respect to energetic costs, this method is more economical than the glass crystallization method [5,12–14], since the latter requires a previous treatment to melt the precursors and also, it is more economical than the methods of reactions in solid state [6–8], sol–gel [9], non-hydrolytic sol–gel [4, 10], and mechanical activation [11] which need higher temperatures to produce cordierite. Moreover, the chlorination of dolomite and kaolinitic clay with chlorine required less amount of time that required for all the processes mentioned above [4–14]. In yet another aspect, the process of chlorination does not need expensive reagents as do the sol–gel [9] and non-hydrolytic methods [4,10].

3.8. SEM and EPMA analysis performed on M sample calcined in Cl_2/N_2

With the aim of corroborating the results obtained through TG and XRD, SEM and EPMA analysis on calcined M sample in Cl_2/N_2 at temperatures of 700 °C and 900 °C and reaction times of 5 and 120 min were carried out. SEM micrographs are shown in Fig. 7 and the results of EPMA analysis performed on the particles shown in Fig. 7b, c and d are presented in Table 5.

Fig. 7a shows SEM image of the product obtained at 700 °C and 5 min. An amplified image (Fig. 7b) of the particle shown in Fig. 7a reveals the presence of needle-shaped particles. The results of microanalysis on particles marked with an arrow indicate that it is mullite, which is one of the products of reaction (5). In Fig. 7c, an agglomerate of particles with heterogeneous shape and formation of pores is observed for the solid chlorinated at same temperature and reaction time of 120 min. According to data obtained through EPMA, the composition of the particles corresponds to that of cordierite. These results corroborate the mechanism proposed for synthesis of cordierite according to Eqs. (5) and (6).

Fig. 7d shows an agglomerate of homogeneous particles and porous for the product of the chlorination carried out at 900 °C and 120 min. By comparing Fig. 7c and d, it can be inferred that the porosity of the particles increases significantly with temperature in the range 700 to 900 °C.

4. Conclusions

1) The results of the chlorination assays of a mixture containing kaolinitic clay and dolomite with the ratio 70/30 (%w/w) have shown that this process is an effective method to produce cordierite at 700 °C and for a reaction time of 120 min. These conditions are below those used in the current processes.
2) The cordierite formation reaction is absolutely selective between 700 and 900 °C.
3) The mechanism of cordierite formation is carried out in two steps. First, the reaction between liquid $MgCl_2$, O_2 and metakaolinite, generating mullite, enstatite and Cl_2 (reaction (5)) occurs. Then, mullite and enstatite are chlorinated producing cordierite, liquid $MgCl_2$ and O_2 (reaction (6)).
4) The iron, present in the mixture as hematite, is removed between 700 and 800 °C for 120 min, and the Fe (III) oxide adsorbed on the surface of kaolinite is eliminated until 0.25% w/w between 800 and 900 °C. There are no considerable changes in the extraction of iron between 900 and 1000 °C. The results obtained by XRF indicate that the removing of iron by chlorination is 88.4% w/w at 900 °C and 88.9% w/w at 1000 °C.
5) The rise of chlorination temperature between 700 and 1000 °C produces a significant increase in the production of cordierite. Moreover, the optimum temperature of chlorination for cordierite synthesis from the raw materials used in this work is 900 °C for two reasons: at this temperature, the iron in the sample is efficiently removed and porous cordierite is selectively produced.
6) The chlorination is a simple and selective process that employs lower temperatures and short reaction times to synthesize cordierite.

Acknowledgments

The authors wish to thank Universidad Nacional de San Luis (UNSL), Fondo para la Investigación Científica y Tecnológica (FONCyT) and Consejo Nacional de Investigaciones Científicas y Técnicas (CONICET) for the financial support.

References

[1] H. Gokce, D. Ağaoğulları, M. Lutfi Ovecoğlu, İ. Duman, T. Boyraz, Characterization of microstructural and thermal properties of steatite/cordierite ceramics prepared by using natural raw materials, J. Eur. Ceram. Soc. 31 (2010) 2741–2747.
[2] A. Yamuna, R. Johnson, Y.R. Mahajan, M. Lalithambika, Kaolin-based cordierite for pollution control, J. Eur. Ceram. Soc. 24 (2004) 65–73.
[3] P. Rohan, K. Neufuss, J. Matjiek, J. Dubsky, L. Prchlik, C. Holzgartner, Thermal and mechanical properties of cordierite, mullite and steatite produced by plasma spraying, Ceram. Int. 30 (2004) 597–603.
[4] I. Janković-Častvan, S. Lazarević, D. Tanasković, A. Orlović, R. Petrović, Dj Janaćković, Phase transformation in cordierite gel synthesized by non-hydrolytic sol–gel route, Ceram. Int. 33 (2007) 1263–1268.
[5] J. Banjuraizah, H. Mohamad, Z.A. Ahmad, Crystal structure of single phase and low sintering temperature of α-cordierite synthesized from talc and kaolin, J. Alloys Compd. 482 (2009) 429–436.
[6] E. Gunay, Sintering behavior and properties of sepiolite-based cordierite compositions with added boron oxide, Turk. J. Eng. Environ. Sci. 35 (2011) 83–92.
[7] N. Obradović, N. Đorđević, S. Filipović, N. Nikolić, D. Kosanović, M. Mitrić, S. Marković, V. Pavlović, Influence of mechanochemical activation on the sintering of cordierite ceramics in the presence of Bi_2O_3 as a functional additive, Powder Technol. 218 (2012) 157–161.
[8] S. Wang, H. Zhou, L. Luo, Sintering and crystallization of cordierite glass ceramics for high frequency multilayer chip inductors, Mater. Res. Bull. 38 (2003) 1367–1374.
[9] A.M. Menchi, A.N. Scian, Mechanism of cordierite formation obtained by the sol–gel technique, Mater. Lett. 59 (2005) 2664–2667.
[10] I. Jankovic-Castvan, S. Lazarevic, B. Jordovic, R. Petrovic, D. Tanaskovic, Dj Janackovic, Electrical properties of cordierite obtained by non-hydrolytic sol–gel method, J. Eur. Ceram. Soc. 27 (2007) 3659–3661.
[11] S. Tamborenea, A.D. Mazzoni, E.F. Aglietti, Mechanochemical activation of minerals on the cordierite synthesis, Thermochim. Acta 411 (2004) 219–224.
[12] G.H. Chen, X.Y. Liu, Sintering, crystallization and properties of $MgOAl_2O_3$–SiO_2 system glass–ceramics containing ZnO, J. Alloys Compd. 431 (2007) 282–286.
[13] A. Goel, E.R. Shaaban, F.C.L. Melo, M.J. Ribeiro, J.M.F. Ferreira, Non-isothermal crystallization kinetic studies on MgO–Al_2O_3–SiO_2–TiO_2 glass, J. Non-Cryst. Solids 353 (2007) 2383–2391.
[14] G.h. Chen, Sintering, crystallization, and properties of CaO doped cordierite-based glass–ceramics, J. Alloys Compd. 455 (2008) 298–302.
[15] Sh.M. Wang, F.H. Kuang, Q.Z. Yan, C.C. Ge, L.H. Qi, Crystallization and infrared radiation properties of iron ion doped cordierite glass–ceramics, J. Alloys Compd. 509 (2011) 2819–2823.
[16] M.A. Camerucci, G. Urretavizcaya, M.S. Castro, A.L. Cavalieri, Electrical properties and thermal expansion of cordierite and cordierite–mullite materials, J. Eur. Ceram. Soc. 21 (2001) 2917–2923.

[17] G. Routschka, Refractory Materials: Pocket Manual: Design, Properties, Testing, Vulkan-Verlag GmbH, Essen, 2008.
[18] I. Gaballah, E. Allain, M. Djona, Chlorination kinetics of refractory metal oxides, Light Met. (1994) 1153–1161.
[19] J.A. González, M. del C. Ruiz, Bleaching of kaolins and clays by chlorination of iron and titanium, Appl. Clay Sci. 33 (2006) 219–229.
[20] J.A. González, A.C. carreras, M. del C. Ruiz, Phase transformations in clays and kaolins produced by thermal treatment in chlorine and air atmospheres, Lat. Am. Appl. Res. 37 (2007) 133–139.
[21] R.P. Orosco, E. Perino, M. del C. Ruiz, J.A. González, A thermogravimetric study of refractory clays chlorination, Int. J. Miner. Process. 98 (2011) 195–201.
[22] P. Orosco, M. del C. Ruiz, J. González, Phase transformations of a talc ore under heated chlorine atmosphere, Thermochim. Acta 554 (2013) 15–24.
[23] F.M. Tunez, J. González, M. del C. Ruiz, Aparato de Laboratorio para Realizar Termogravimetrias en Atmosferas Corrosivas y no Corrosivas, 2007. (P060100450).
[24] C. Robelin, P. Chartrand, A.D. Pelton, ($MgCl_2 + CaCl_2 + MnCl_2 + FeCl_2 + CoCl_2 + NiCl_2$) system, J. Chem. Thermodyn. 36 (2004) 793–808.